Chinese Society of Pavement Engineering
International Journal of
Pavement Research and Technology
Journal homepage: www.springer.com/42947

Effect of wetting and drying on the resilient modulus and permanent strain of a sandy clay by RLTT

Frank Siaw Ackah, Nie Zhuochen, Feng Huaiping*

State Key Laboratory of Mechanical Behavior and System, Safety of Traffic Engineering Structures, Shijiazhuang Tiedao University, Shijiazhuang, 050043, China

Received 27 March 2020; received in revised form 30 August 2020; accepted 1 September 2020; available online 19 September 2020

Abstract

Water content is one of the significant factors that affect the stability and stiffness property of the subgrade soils. Under changing environmental conditions such as raining and drought, the water content becomes more variable and is known to facilitate many of the subgrade-related problems such as rutting and swelling. As a result, the compaction moisture and post-compaction moisture changes on the resilient modulus (M_R) and permanent strain (ε_p) of a subgrade soil were investigated. The effect of the bulk stress, octahedral shear stress, wetting, and drying was analyzed using test results and has important consequences on the existing and design of new pavements. M_R was higher for soil samples subjected to drying than wetting. Higher M_R did not show lower ε_p. The correlation between M_R and ε_p suggests that M_R was not a satisfactory soil property to explain ε_p of the soil in the Ciyaowan station in Bao-shen. Models used to predict the effect of the moisture content, and stress state showed better performance for M_R.

Keywords: Resilient modulus; Permanent deformation; Water content; Subgrade soil

1. Introduction

The moisture content and its variation are among the several relevant factors that compromise the performance of the subgrade. The moisture content of the subgrade layer varies with the rate of infiltration of rainwater, the variation of the level of groundwater table, the migration of moisture between the layers due to temperature variations, evapotranspiration, seasonal variation and the use of inadequate moisture content during compaction, etc. The effect of the moisture content and its variation on M_R have been well researched and documented [1-3]. From the aforementioned, it is evident that moisture content and its variations must be taken into consideration when selecting M_R for pavement design.

M_R is broadly defined as the elastic modulus (stress divided by recoverable strain) after the material has sustained some level accumulated ε_p It is the significant property for the characterization of repeated loading behaviours of subgrade, subbase, and base course materials in pavement structures. M_R represents the mechanical property of the material's ability to resist deformation under stress. The American Association of State Highway and Transportation Officials (AASHTO) software, AASHTOWare, Mechanistic-empirical pavement design guide (MEPDG), requires the M_R as a primary material property for subgrade soils, subbase course, and base course. However, research studies show that some cohesive soils yield significantly under service loads. Soils may exhibit higher M_R and yet still yields. [4,5]. Though the M_R is low at high moisture content and vice versa, it necessary to determine the M_R and ε_p of soil considering moisture content variation under changes of wetting and drying conditions especially for mixed soils. This would be valuable for the proper design and evaluation of pavement structures. M_R and ε_p are the most important parameters for the design of pavements against pavement distress such as roughness and rutting [6,7]. Failure to include it can lead to higher annual rehabilitation costs and significant passenger discomfort during the service period of the rail or road infrastructure.

Several studies have addressed the influence of moisture content changes on M_R by looking at the variations in compaction moisture content/degree of saturation, suction, and post-compaction due to wetting and drying. Models have been established to also describe the resilient modulus with respect to the water content [8]. [2] evaluated the effect of post-compaction moisture content on the M_R of subgrade soils and modified MEPDG recommended M_R–moisture model. [9] investigated the seasonal moisture variation on the M_R of Brazilian soils. A series of other separated studies have also been conducted to evaluate other factors on M_R Stress [10], material properties [11], measurement methods [12,13] and climatic impacts [14,15] whiles others researched the relationships between M_R test methods [16-19], the effect of testing protocols [20], relationship between laboratory M_R and M_R back- calculated

* Corresponding author
E-mail address: fhping234@outlook.com (F. Huaping).
Peer review under responsibility of Chinese Society of Pavement Engineering.

ISSN: 1997-1400 DOI: https://doi.org/10.1007/s42947-020-0067-3
Chinese Society of Pavement Engineering. Production and hosting by Springer Nature

from non-destructive test methods [21]. However, the compaction moisture and post compaction moisture content effect considering M_R and ε_p have not been considered.

ε_p, is influenced mainly by load-related factors that relate to material properties [22-24]. Load-related factors that encompass the applied stress levels, number and loading history, and material strength [25,26].Significant material properties that affect ε_p include moisture content, matric suction, degree of compaction, gradation properties, percentage passing sieve number 200 or 0.075-mm, the type of fines, particle morphology, and aggregate mineralogy [2,17,27]. Significant literature on ε_p models [4,5,28]. Laboratory test methods such as dynamic and cyclic triaxial tests, simple and cyclic shear tests, resonant column and hollow cylinder tests, and among others have been used to determine permanent deformation. The above testing procedures were also used to determine shear stress-strain behaviour, M_R of subgrade, etc. Test results were used to assess the elastic and plastic deformation. Plastic deformation is usually described by non-linear elastic models, however, ε_p is complex, it depends on the accumulation of N loading cycles. At the laboratory, one of the most widely used test methods for examining M_R and ε_p is the M_R test from the repeated load cyclic triaxial test.

In view of the recent interest in implementing the modulus base compaction control by most countries, improving the performance of the compacted subgrade, this study was conducted to add to the understanding and contributions on the progress made on the impact of the wetting and drying on M_R and ε_p properties of sandy clayey soils.

2. Materials and methodology

Locally available soils, taken from the field site of Ciyaowan station in Bao-Shen, were used to study the post compaction moisture effect on the M_R and ε_p. The soil was a grey-brown soil with blotches of red, slightly plastic and has variable percentages of coarse sand. Standard laboratory tests were conducted to classify the soils and also to determine the basic physical properties. The soil is described as ML according to the Unified Soil Classification System of the American Society of Testing and Materials (ASTM 2006), and as A-2-6 following the American Association of State Highway and Transportation Officials (AASHTO 2000) protocols. Fig. 1 shows the particle-size distribution. Table 1. Summarizes the properties.

2.1. Specimen preparation

Before M_R test, samples were subjected to equal sample preparation procedures. Preparation procedures include breaking off lump soils, mixing oven-dried soil samples with water, and compaction of soil specimen. First soil lumps were broken, soils were first kept in an oven at a temperature of 105°C for 24hrs. Afterward, soil samples were allowed to cool for a day. The required amount of dried soil and water was calculated and mixed together in a bowl. The mixture was later transferred into an airtight container and stored at room temperature for 24hrs for moisture equilibration. Before compaction, the soil was mixed together to ensure uniform distribution of soil moisture content. Samples were compacted in four equal layers on the bottom platen inside a split mold using the impact procedure. Samples were compacted at 95% to 100% maximum dry density (MDD) (1.84gcm^{-3}) to reduce the effect of density on a tested specimen. The sample sizes were 39.1 mm in diameter and 80 mm in height.

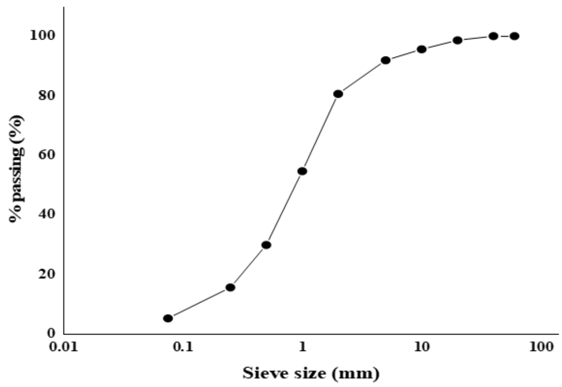

Fig. 1. Grading characteristics.

Table 1
Index properties of the soil.

Property	Measured value
Maximum dry density (MDD) (g/cm^3)	1.84
Optimum moisture content (OMC) (%)	11
Coefficient of uniformity	8.86
Coefficient of curvature	1.44
Specific gravity	2.68
Atterberg limits (grain size <425 m)	
Liquid limit (%)	32.2
Plastic limit (%)	20.9
Plasticity index (%)	11.3

2.2. Wetting and drying procedure

Various laboratory procedures have been used for wetting and drying of compacted subgrade soils. This study adopted [29]. Samples were separated into group's Table 2. The wetting procedure involves putting the specimen in a triaxial cell and applying 27.6 kPa of confining pressure; whiles injecting the required volume of water from the bottom with a pressure of 13.78 kPa, then applying a vacuum pressure of about 13.3 kPa (1.9 psi, 100 mm Hg) for an hour. Afterward, the specimen is placed in a vacuum for about 24hrs before M_R.

The drying procedure involves wrapping the specimen in a rubber membrane after compaction and inserting a circular plastic sheet at the end of the specimen. Afterward, two platens were placed over the plastic sheets i.e one at the bottom and other the top and sealed off the membrane from the platens with masking tape. The complete setup was then put in an oven at 41°C (105°F) and weighed at designated time intervals until the desired weight was achieved. The samples were then placed in an airtight container for 48hours before testing.

After the M_R test, moisture changes across the height of the specimen were determined by slicing the specimen into four slices and then tested for moisture variation using the gravimetric method. The moisture distribution throughout the radius and height varied by ±5 % and is generally acceptable.

2.3. M_R test procedure

A computer-controlled dynamic triaxial testing system (2Hz/5Hz/ 10Hz DYNTTS) was used. M_R test was conducted in accordance with AASHTO T307-99 procedures. Samples were first preconditioned up to 1000 load cycles to minimize the

Table 2
Sample grouping for M_R and ε_p test.

Group	Sample preparation and conditioning.	Purpose
Group 1	Samples prepared at OMC, OMC -4%, OMC+4%	Samples will be used to assess the effect of the compaction moisture content. As reference for assessing the post compaction moisture effect on M_R and ε_p
Group 2	Samples prepared at OMC+4%, dried to OMC and OMC+4%	For assessing the effect drying on samples prepared at OMC+4
Groups3	Samples prepared at OMC -4%, wetted to OMC and OMC+4%	For assessing the effect of wetting on samples prepared at OMC-4%
Group 4	Samples prepared at OMC dried to OMC-4%	For assessing the effect of drying on samples prepared at OMC

imperfections in contact between end platens and specimens. The cyclic haversine-shaped load plus with a duration of 0.1 seconds and a rest period of 0.9 seconds was used. During testing, the strain measured was used to derive plastic deformation and elastic strain Fig. 2. Plastic deformations were used to determine $\epsilon_p$and elastic strain used to determine M_R. In all the load sequence, the applied load and the vertical displacement for the last five cycles were used to determine the M_R and ε_p. In all, a total of 16 load sequences were applied Table 3. To ensure repeatability and reliability test results, tests were conducted on similar specimens prepared in similar conditions. A total of two identical samples were tested for this assessment. Results were compared and the average used for this study, test results did not vary much (±5%). Fig. 3 shows the experimental setup.

2.4. Soil water characteristics (SWCC) test

Fig. 4 was determined using the pressure plate apparatus. Experimental steps mainly involved sample preparation, ceramic

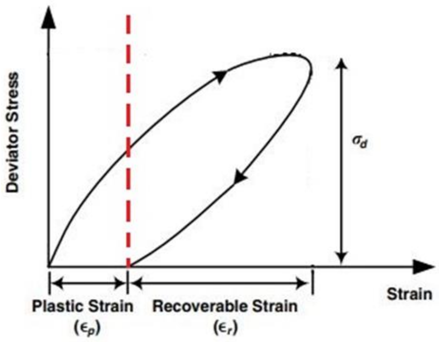

Fig. 2. Determination of the M_R and ε_P.

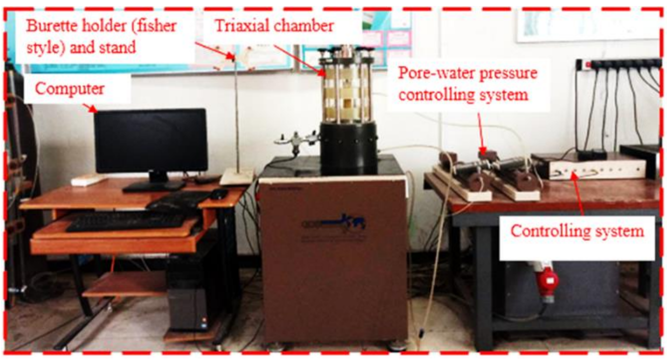

Fig. 3 GDS system used for the M_R test.

Table 3
Loading sequence for the resilient modulus test AASHTO T307.

Sequence	Confining pressure (KPa)	Max Axial stress (KPa)	Cyclic stress (KPa)	Constant stress	No of load application
0	41.4	27.6	24.8	2.8	1000
1	41.4	13.8	12.4	1.4	100
2	41.4	27.6	24.8	2.8	100
3	41.4	41.6	37.3	4.1	100
4	41.4	55.2	49.7	5.5	100
5	41.4	68.9	62.0	6.9	100
6	27.6	13.8	12.4	1.4	100
7	27.6	27.6	24.8	2.8	100
8	27.6	41.4	37.3	4.1	100
9	27.6	55.2	49.7	5.5	100
10	27.6	68.9	62.0	6.9	100
11	13.8	13.8	12.4	1.4	100
12	13.8	27.6	24.8	2.8	100
13	13.8	14.4	37.3	4.1	100
14	13.8	55.2	49.7	5.5	100
15	13.8	68.9	62.0	6.9	100

disk saturation, and data reading. The test began with saturating the ceramic disk by immersion in water (24hrs). The disk was removed and installed in the pressure plate with a soil sample prepared to the MDD (A sample prepared with 2cm-high cutting ring with an area of 30cm^2 and an inner diameter of 61.8 mm, and then saturated using the vacuum saturation) on the disk. An outlet provided in the water compartment below the ceramic disk where water can drain from the soil specimen was connected with a piece of tubing that connects to a burette. The pressure plate is covered with a lid and properly closed tightly. The system is then checked for accurate installations, checked for air leakages, etc. The required amount of pressure levels were then applied. Pressure levels were allowed to reach levels that were only required to avoid problems normally associated with hysteresis. The required pressure is then sustained in the pressure plate device until the water level in the burette becomes static and this normally takes time, at times days. More time may be required at very low pressures. The matric suction was established by correlating pressures with the corresponding volume. The volume of water loss was determined by removing the sample from the apparatus and quickly weighing. Samples were then placed back in the pressure plate apparatus. Applied matric suction was equivalent to the applied pore air pressure. The process is repeated until all suction steps were complete. A very high air entry value ceramic disk was used.

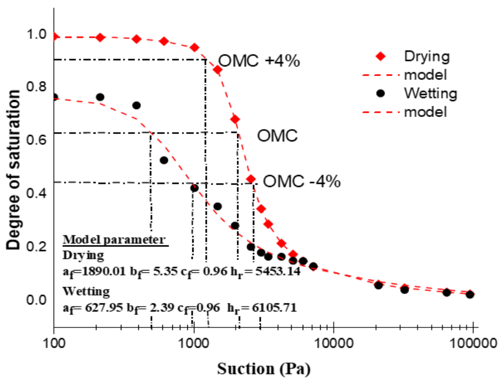

Fig. 4. Soil water characteristics curve.

To determine wetting path, pore air pressure was reduced from the highest matric suction, whiles keeping water pressure at the constant value of zero. This enables water to flow into the sample through the ceramic disk. Subsequently, the pressure levels are reduced gradually at the desired pressure levels, similar technique adopted in the drying process is adopted to obtain the corresponding volume change and the applied pressure. The process is repeated until the samples become fully saturated, and zero matric suction is achieved. The total moisture content was determined by oven - drying the sample. Actual water content at each suction level was calculated using the final moisture content and the weight of the sample at various suction levels of soil. Once the SWCC$_s$ was established, results were fitted to Fredlund and xing's models (1) to establish a relationship between soil suction and saturated water content.

$$S_s = C(\Psi) \times \frac{S_s}{\{ln[exp(1)+(\Psi/\alpha_f)^{bf}]\}^{cf}}, C(\Psi) = 1 - \frac{\ln\left(1+\left(\frac{\psi}{h_r}\right)\right)}{\ln\left(1+\left(\frac{10^6}{h_r}\right)\right)} \quad (1)$$

where, $S_s$the of degree of saturation; S_s is the saturated; ψ is soil suction; a_f, b_f, c_f, and h_r are model parameters and are primary functions of the air entry value, rate of water extraction, residual water content and suction at residual water content, suction at which residual water content occurs.

3. Result and discussion

[5,30] have emphasized the need of testing unbound pavement materials for ε_p behaviour along with commonly used M_R test procedures. This is necessary because the ε_p properties of unbound soil materials and M_R behaviour of unbound materials are not necessarily proportional. ε_p characteristics are key factors when it comes to pavement failure.

3.1. Resilient modulus

There appears to be a non-linear trend for the M_R and maybe as a result of an inadequate instrumental resolution that occurs at very high specimen stiffness associated with water contents Fig. 5, Fig. 6, and Fig. 7. Further, it can also be related to the water content in the specimen becoming more variable. According to [31] this can be a result of the small pore spaces. M_R values for sample compacted at Optimum moisture content (OMC) (11.1%) at MDD (1.84g/cm^3) were between 131.24 MPa and 166.69 MPa, which is similar to results that were reported by [13,32] for similar soils.

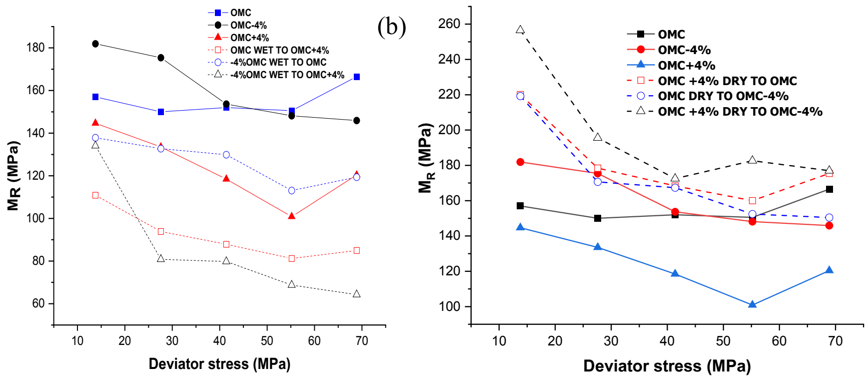

Fig. 5 Effect of the deviator stress on the resilient modulus at a confining pressure of 41.4 KPa considering (a) wetting and (b) drying.

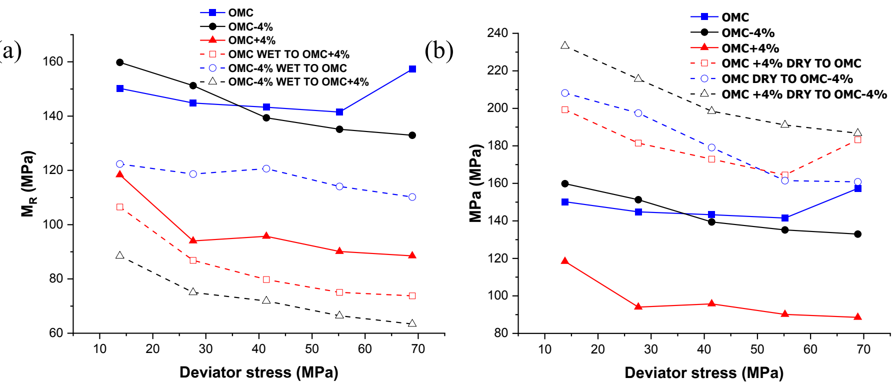

Fig. 6 Effect of the deviator stress on the resilient modulus at a confining pressure of 27.6 KPa considering (a) wetting and (b) drying.

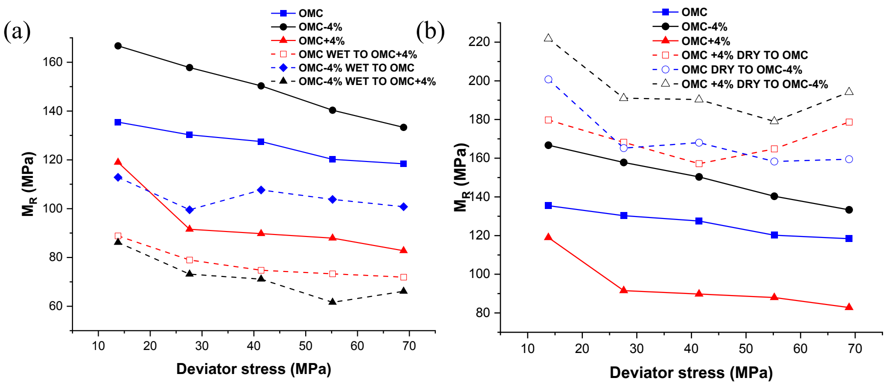

Fig. 7. Effect of the deviator stress on the resilient modulus at a confining pressure of 13.8 KPa considering (a) wetting and (b) drying.

3.2. M_R moisture relationship

Moisture contents were within 7.1% and 15.1% signifying that M_R of this material may increase or even decrease at water contents ±11.1%. Comparing the M_R values of samples compacted at OMC and OMC-4% showed an increase in about 5.93% of M_R while samples compacted at OMC+4% resulted in about 26.55% decrease of the M_R considering the average M_R. From the result, it is realized that M_R is more sensitive to the moisture content effect. These behaviours are typical for fine-grained soils and similar observations were found [2,2,14,33]. Fig. 8 indicates that maximum M_R was recorded for samples subjected to lower moulding moisture contents. The decreased M_R values with increased moisture content can be attributed to the weakening of the soil fabric as moisture content increases. This can also appear to have been caused by capillary suction and lubrication. M_R increases with a decrease in moulding moisture content. An explanation of this behaviour could be that the soil becomes stiffer as the water content decreases, high inter-particle forces between particles and low lubrication. Similar observations have been reported by [1,34].

3.3. Effect of the drying and wetting on M_R

Fig. 9 shows that the wetting and drying processes were accurate and can be used to predict the post compaction moisture for the bulk samples. The M_R–moisture content relationships for specimens compacted at different moisture content and then dried to a lower moisture content are determined and presented in Fig. 10. From the test results, increased or prolonged drying did not increase in M_R much. Similar observations were made by

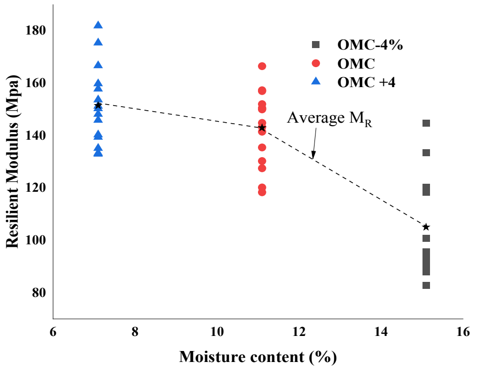

Fig. 8. Effect of the compaction moisture content on M_R.

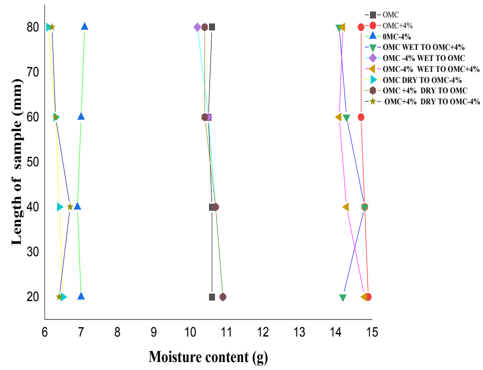

Fig. 9. Moisture variation along the length of the sample.

[2,29,35,36] stipulated that such behaviour is similar to the hysteresis of the SWCC. It indicates that both the initial moisture content and the extent of drying are important factors. From the results, it can be said that when a given soil is sufficiently dried, more drying would cause less increase in M_R [1].

The effect of wetting was significant Fig. 10. Comparing the M_R of a specimen prepared at OMC, OMC-4%, and OMC+4% to specimens subjected to wetting. Results indicate that there was a significant decrease in the M_R of samples subjected to wetting conditions. From this, it can be concluded that the initial moisture content and the extent of wetting is also an important factor and results conform to the results reported elsewhere [3,29]. An explanation to this could be that an increase in moisture content

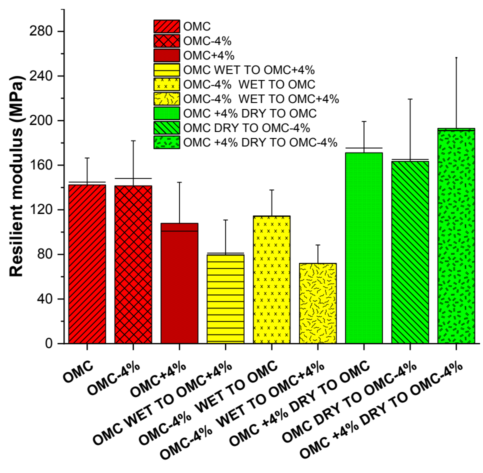

Fig. 10. Effect of the wetting and drying on M_R.

reduces the cohesion strength of the soils with a lubricating effect that reduces the soil M_R. This can also be explained by suction hysteresis Fig. 4. It is obvious that suction values of samples subjected to the wetting and drying conditions will be lower or higher depending on the extent of wetting and drying conditions, and the initial moisture content. From literature, lower suction values are normally associated with samples subjected to wetting conditions and vice versa [37]

3.4. Permanent deformation from the resilient modulus test

For most of the soils tested, small ε_p occurred. Samples subjected to wetting conditions showed excessive ε_p for the first 1000 cycles Table 4. Very high initial strain recorded for the samples prepared and tested at OMC-4% wet to OMC+4% may be the result of imperfections at the bottom of the samples. Plastic strains measured after the first 1000 cycles were generally smaller and lower for soils with low moisture content. Higher ε_p were measured at preconditioning stages for all the samples and samples subjected to wetting conditions.

Fig. 11 shows the relationship between M_R and ε_p for all the tested samples at the different moisture contents and post compaction moisture contents. Higher M_R consistently did not show lower ε_p for all the samples and agree well with [4,5] observations. A low coefficient of determination (R^2) was observed for the relationship between the M_R and ε_p. The poor correlation between M_R and ε_p suggests that M_R is not a satisfactory soil property to explain ε_p and this is contradictory to [38] observation for coarse-grain soils and further explains the complex behaviour of cohesive soils.

3.5. Resilient modulus models.

There are a number of models for predicting the effect of various influencing factors on M_R. MEPDG recommends Eq. (2) to describe the stress state effect, and Eq. (6) describes the variation of the M_R with saturation taken into account the influence of moisture content. However, Eq. (2) and Eq. (6) are empirical relationships that describe conditions that better assured the performance of pavement in pavement construction. Fig. 12 shows the wetting and drying path predicted with Eq. (3) and further fitted with an improved model Eq. (7). It can be seen from Fig. 12, the MEPDG model could not accurately predict the moisture relationship. Eq. (7) a model developed [10] predicted well with R^2 of 0.71 and Km 2. 854.

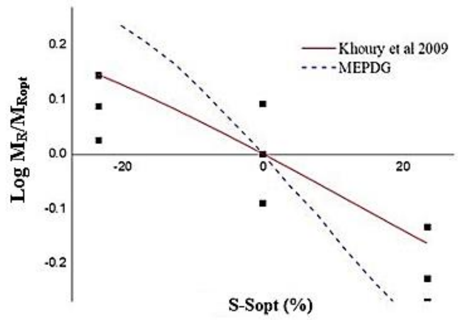

Fig. 11. M_R–moisture relationship as in construction practice considering post wetting and drying effect.

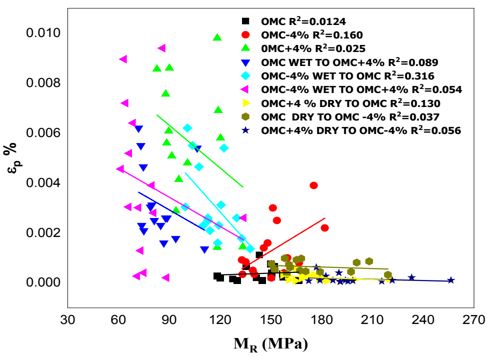

Fig. 12. Correlation between M_R and ε_p.

To evaluate the effect of stresses as in pavement construction practice, all test results were fitted with Eq. (2), to assess the dilation effect that occurs during testing, results were also fitted with Eq. (4) and further fitted with Eq. (3) to assess the effect of other stress variables on M_R. All the models show a good coefficient of determination (R^2). The performance offered by Eq. (4) is almost the same as the others. [10,39] concluded that Eq. (4) has advantages of reducing the softening and hardening effect. It also reduces computational time when used for numerical analysis. Comparing the model results, it is evident that the test method used to establish permanent deformation was limited to the dilational effect [30] that normally affects the test method. Model parameter k_1 was used to characterize the stiffness of the subgrade soil and is directly proportional to the M_R. $k1$ increases with an increase in effective stress and decreases with an increase in moisture content Eq. (8).

Table 4
ε_p model parameters and the initial ε_p.

Sample ID	α_1	α_2	α_3	α_4	R^2	Initial ε_p (%)
Initial compaction moisture						
OMC	0.761	-0.852	0.664	-1.366	0.127	0.029
OMC+4%	0.769	-0.813	-0.914	1.066	0.23	0.0435
OMC-4%	0.846	-0.321	2.605	-3.843	0.673	0.5849
Wetting Conditions						
OMC WET TO OMC+4%	0.749	-0.894	-0.909	1.256	0.424	0.243
OMC-4% WET TO OMC	0.759	-0.811	-0.839	1.679	0.605	0.152
OMC-4% WET TO OMC+4%	0.761	-0.799	0.523	2.239	0.239	1.208
Drying conditions						
OMC DRY TO OMC-4%	0.73	-1.022	-0.68	0.612	0.311	0.0974
OMC+4% DRY TO OMC	0.723	-1.117	-0.389	0.051	0.096	0.0474
OMC+4 DRY TO OMC-4%	0.722	-1.131	0.263	0.805	0.096	0.1404

Eq.(8) derived by substitution of Eq. (2) into Eq. (6). From Eq. (8) it can be seen that the MEPDG moisture correction model (Eq. (6)) that the change in moisture conditions affects k_1 model parameter but does not affect k_2 and k_3. However, for k_1 to better assure the performance of the subgrade, the moisture content must be in its right proportions (OMC). k_2 reflects on the influence of confining pressure (minimum bulk stress) on M_R and is directly associated with confining pressure. It produces a stiffening effect on the material and the higher it is, the higher the M_R. The value of k_3 is negative, indicating a negative correlation between the M_R and the octahedral shear stress. k_3 shows that the M_R of subgrade soils decreases with an increase in shear stress. Fig. 13 shows the predicted and measured M_R for Eq. (2), Eq. (3), and Eq. (4). It is realized that most of the samples were close to the line of equity. Table 5. Summarizes the model results.

$$M_R = P_a k_i \left(\frac{\theta}{P_a}\right)^{k_2} \left(\frac{\tau_{oct}}{P_a} + 1\right)^{k_3} \tag{2}$$

$$M_R = k_1 P_a \left(\frac{\delta_3}{P_a} + 1\right)^{k_2} \left(\frac{\delta_d}{P_a} + 1\right)^{k_3} \tag{3}$$

$$M_R = P_a k_i \left(\frac{\theta_m}{P_a}\right)^{k_2} \left(\frac{\tau_{oct}}{P_a} + 1\right)^{k_3} \tag{4}$$

where, for repeated load triaxial test (RLTT), $\sigma_2 = \sigma_3$ which is equal to confining pressure, $\sigma_1 = \sigma_3 = +q$ where q is the maximum deviator stress. Bulk stress $(\theta) = \sigma_3 + \sigma_2 + \sigma_3, or\ 3\sigma_3 + \sigma_d = \theta$. Minimum bulk stress $\theta_m = \theta - \sigma_d$, τ_{oct} is octahedral shear stress. k_1, k_2 and k_3 are regression coefficient/model constants. P_a reference atmospheric pressure, δ_3 minor principal stress or confining pressure; δ_d deviatoric stress

$$\tau_{oct} = \sqrt{(\sigma_1 - \sigma_2)^2 + (\sigma_2 - \sigma_3)^2 + (\sigma_3 - \sigma_1)^2/3} \tag{5}$$

$$log\left(\frac{M_R}{M_{Ropt}}\right) = a + \frac{b-a}{1+e^{ln\left(\frac{-b}{a}\right)+K_m(S-S_{opt})}} \tag{6}$$

$$log\left(\frac{M_R}{M_{Ropt}}\right) = a + \frac{b-a}{1+exp\left(ln\left(\frac{-b}{a}\right)+K_m(S-S_{opt})\right)},\ K_m = 0.375PI \tag{7}$$

$$M_R = 10^{a+\frac{b-a}{1-\exp[k_m(S-S_{opt})}} k_1 P_a \left(\frac{\theta}{P_a}\right)^{K_2} \left(\frac{\tau_{oct}}{P_a} + 1\right)^{k_3} \tag{8}$$

M_R = at any given moisture content; M_{Ropt} = M_R at optimum Moisture content; $\frac{M_R}{M_{opt}}$ M_R ratio; a = minimum of $log\left(\frac{M_R}{M_{opt}}\right)$, b=maximum of $log\left(\frac{M_R}{M_{opt}}\right)$, k_m = regression parameter; and $S - S_{opt}$ = variation of degree of saturation, expressed as a decimal, k_1, k_2 and k_3 are regression coefficient/model constants. P_a reference atmospheric pressure. Fig. 9 shows the wetting and drying path.

Table 5
M_R model parameters.

Moisture Content/%	Universal model				Zhang et al 2018				Ni et al 2002			
Initial compaction moisture content												
	k_1	k_2	k_3	R^2	k_1	k_2	k_3	R^2	k_1	k_2	k_3	R^2
OMC	1521.21	0.26	-0.61	0.67	1514.07	0.19	-0.042	0.79	1125.97	0.92	-0.03	0.76
OMC-4%	1846	0.09	-1.23	0.78	1837.49	0.06	-1.03	0.77	1682.9	0.34	-0.57	0.8
0MC+4%	1417.23	0.36	-2.1	0.7	1408.11	0.25	-1.34	0.72	972	1.32	-0.75	0.78
`Wetting Conditions												
OMC WET TO OMC+4%	1124.36	0.22	-1.88	0.87	1116.7388	0.16	-1.39	0.77	898.37	0.79	-0.77	0.88
OMC -4% WET TO OMC	1353.29	0.26	-1.13	0.89	1342.86	0.17	-0.57	0.87	1044.98	0.87	-0.31	0.87
OMC-4% WET TO OMC+4%	1197.93	0.294	-2.93	0.72	1181.71	0.18	-2.29	0.69	909.87	0.99	-1.27	0.72
Drying conditions												
OMC+4% DRY TO OMC	2055.81	0.12	-1.02	0.56	2044.24	0.08	-0.75	0.54	1838.14	0.39	-0.42	0.55
OMC DRY TO OMC -4%	2224.55	0.03	-1.45	0.78	2219.13	0.02	-1.37	0.77	2198.13	0.08	-0.76	0.78
OMC+4% DRY TO OMC-4%	2453.03	0.03	-1.25	0.63	2444.09	0.02	-1.16	0.62	2422.49	0.074	-0.65	0.63

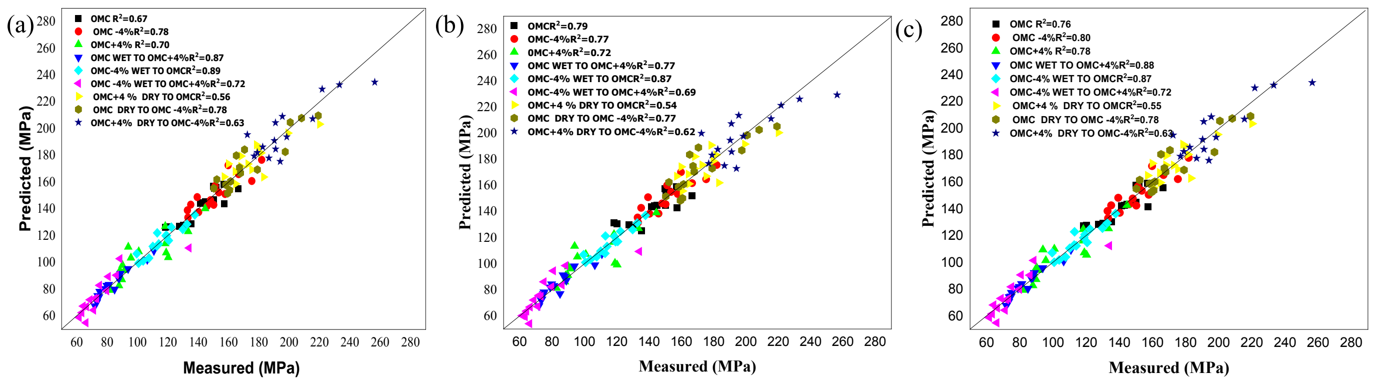

Fig. 13. Predicted M_R versus measured M_R (a) universal model (b) Ni et al model 2002, and (c) Zhang et al 2018 model.

3.6. Permanent deformation model

Several models are available for assessing ε_p of the unbound pavement materials. However, in this study, the four-parameter model proposed by [4] and classical power law was used.

$$\varepsilon_p = \alpha_1 N^{\alpha_2} \left(\frac{\delta_{oct}}{P_a}\right)^{\alpha_3} \left(\frac{\tau_{oct}}{P_a}\right)^{\alpha_4} \quad (9)$$

where, δ_{oct} is octahedral normal stress $(\delta_d+3\delta_3)/3$, τ_{oct} is the octahedral shear stress, N=number of load application, α_1, α_2, α_3, and α_4 are model constants,

Almost all the test results showed a poor coefficient of determination. Table 4 shows the model parameters. Fig. 14 shows the results of measured and predicted values and was not close to the line of equity. Model parameter α_1 indicates that the ε_p are positively correlated with the number of loading cycles. The coefficients α_3 and α_4 shows that ε_p are influenced by both octahedral normal and shear. The inconsistency in positive and negative values recorded for the coefficients related to octahedral stress, normal stress clearly suggest the behaviour of these soils under varying moisture conditions.

3.7. Effect of wetting and drying on pavement performance

To account for the performance of the subgrade soil considering, wetting, and drying, a hypothetical road pavement section Fig. 15 was used. The KENLAYER program [40] was used to model the components of the pavement structure. Layer properties are summarized in Table 6. The non-linear analysis made involved the determination of the vertical compressive strain on top of the subgrade and the horizontal tensile strain beneath the asphalt layer for rutting failure. The average M_R's were used to represent the M_R of the subgrade soils and the k_1 parameter was obtained from (Eq. (2)).

From the analysis, there was a change of the vertical displacement Table 7, vertical stress Table 8, major stress Table 9, vertical strain Table 10, principal strain Table 11, Minor principal strain Table 12 along with the vertical coordinates for the different points (10 points) and are influenced by the depth of the coordinates. The maximum vertical compressive stress observed was 53.692KPa (OMC) and the minimum was 0.734KPa (OMC -4% WET TO OMC; OMC+4% DRY TO OMC; OMC DRY TO OMC -4%; OMC+4% DRY TO OMC-4%). It was also observed that the results of the vertical compressive strains varied marginally for all the different moisture conditions and were dependent on the zone of influence. A comparison of the horizontal tensile strain beneath the asphaltic layer and vertical compressive strain on top of the subgrade for the different moisture conditions is also presented Fig. 16 for rutting potential. Higher vertical strains on top of the subgrade are generally associated with the increase in rutting potential from permanent deformation whiles higher tensile strain beneath asphaltic layer increase rutting potential by fatigue failure. Rutting is reduced for OMC samples considering the vertical compressive strains on the top of the subgrade. This may be the result of the right proportions of the soil moisture content. A higher value was recorded for OMC-4% WET TO OMC+4%. Comparing results of OMC -4% WET TO OMC and OMC-4% WET TO OMC+4% as well as the results of OMC+4% DRY TO OMC and OMC+4% DRY TO OMC-4%, we observed increase of 17.37% and 138.53% respectively. Signifying that the extent of wetting and drying has a significant impact on rutting potentials. Further, comparing the results of OMC, OMC-4%, and OMC+4%, it was realized that OMC recorded the least vertical strain on the top of the subgrade layer.

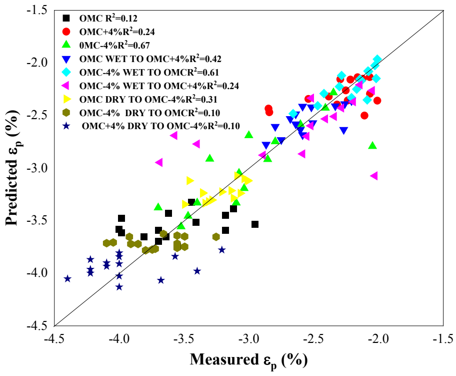

Fig. 14. Predicted ε_p versus measured ε_p.

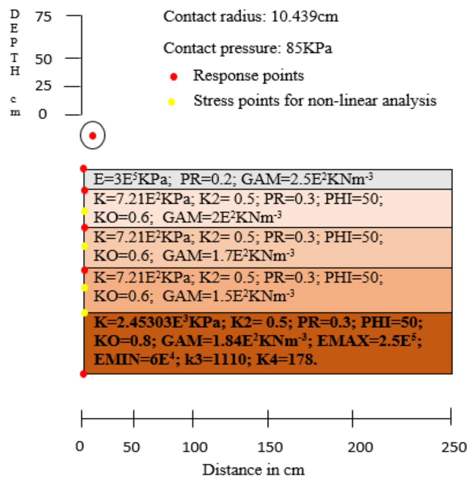

Fig. 15. A systematic model of pavement system with response poInter.

Table 6
Design parameters for damage analysis.

Layer (Material type)	Thickness (cm)	Elastic modulus (KPa)	Poisson ratio	Density (gcm^{-3})
Surface Course (Asphalt Concrete Mixture)	10.16	3.000E+05	0.2	2.5
Base Course (Asphalt Treated)	15.24	2.500E+05	0.3	2.0
Unbound Aggregate base course	15.24	2.000E+05	0.3	1.7
Unbound sub base	30.48	1.400E+05	0.3	1.5
Subgrade		Average M_R values from test results	0.3*, 0.45	1.84

*unsaturated samples.

Comparing the results of the tensile strain beneath the asphaltic layer of OMC -4% WET TO OMC and OMC-4% WET TO OMC+4% showed 2.258E-4 for the two conditions. A similar comparison between OMC+4% DRY TO OMC and OMC+4% DRY TO OMC-4% showed 1.866E-4 and 2.258E-4 respectively. This implies that, under different drying and wetting conditions the rutting potentials can be as a result of the vertical compressive strains from the subgrade for the former and the latter a combination of the tensile strains beneath the asphaltic layer and vertical compressive strains on top of the subgrade layer.

Assessing the results, it can be concluded that the effect of drying and wetting has a profound effect on the extent of rutting potentials and dictates the potential cause of rutting in flexible pavements.

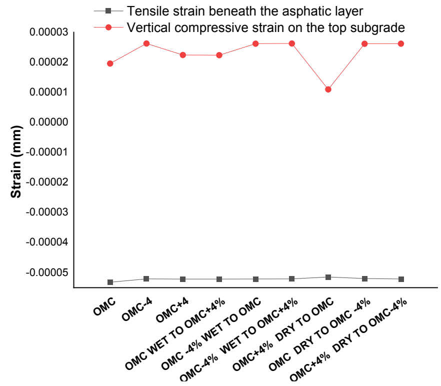

Fig. 16. Variation of vertical compressive strain and tensile strain for rutting potentials.

Table 7
Variation of Vertical displacement with depth.

Vertical coordinates (Depth) cm	OMC (mm)	OMC+4 % (mm)	OMC-4% (mm)	OMC WET TO OMC+4% (mm)	OMC-4% WET TO OMC (mm)	OMC-4% WET TO OMC+4% (mm)	OMC DRY TO OMC-4% (mm)	OMC+4% DRY TO OMC (mm)	OMC+4 DRY TO OMC-4% (mm)
0	0.00755	0.0083	0.0083	0.0083	0.00829	0.0083	0.00828	0.00826	0.00829
10.16	0.00482	0.00559	0.00559	0.00558	0.00557	0.00558	0.00557	0.00556	0.00557
10.16254	0.00482	0.00559	0.00559	0.00558	0.00557	0.00558	0.00557	0.00556	0.00557
25.4	0.00267	0.00345	0.00353	0.00344	0.00344	0.00344	0.00343	0.00343	0.00344
25.40254	0.00267	0.00345	0.00345	0.00344	0.00344	0.00344	0.00343	0.00343	0.00344
40.64	0.002	0.00279	0.00345	0.00279	0.00278	0.00279	0.00278	0.00278	0.00278
40.64254	0.002	0.00279	0.00279	0.00279	0.00278	0.00279	0.00278	0.00278	0.00278
71.12	0.00157	0.00234	0.00279	0.00236	0.00236	0.00234	0.00236	0.00236	0.00236
71.12254	0.00157	0.00236	0.00236	0.00236	0.00236	0.00236	0.00236	0.00236	0.00236
106.68	0.0011	0.00172	0.00178	0.00178	0.00172	0.00172	0.00171	0.00172	0.00172

Table 8
Variation of vertical stress depth.

Vertical coordinates (Depth) cm	OMC (KPa)	OMC+4 % (KPa)	OMC-4% (KPa)	OMC WET TO OMC+4% (KPa)	OMC-4% WET TO OMC (KPa)	OMC-4% WET TO OMC+4% (KPa)	OMC DRY TO OMC-4% (KPa)	OMC+4% DRY TO OMC (KPa)	OMC+4 DRY TO OMC-4% (KPa)
0	85	85	85	85	85	85	85	85	85
10.16	53.692	53.641	53.651	53.661	53.665	53.655	53.633	53.419	53.665
10.1625	53.682	53.631	53.641	53.651	53.655	53.645	53.622	53.409	53.655
25.4	18.482	18.29	19.502	18.326	18.343	18.319	18.337	18.293	18.344
25.4025	18.478	18.286	18.302	18.323	18.34	18.316	18.334	18.291	18.34
40.64	8.02	7.717	18.299	7.693	7.726	7.715	7.729	7.715	7.726
40.6425	8.019	7.716	7.682	7.692	7.725	7.714	7.728	7.714	7.725
71.12	1.945	1.452	7.681	1.467	1.484	1.451	1.484	1.484	1.484
71.1225	1.945	1.489	1.47	1.467	1.484	1.487	1.484	1.484	1.484
106.68	0.913	0.736	0.779	0.778	0.734	0.735	0.734	0.734	0.734

Table 9
Variation of the major principal stress with depth.

Vertical coordinates (Depth) cm	OMC (KPa)	OMC+4 % (KPa)	OMC-4% (KPa)	OMC WET TO OMC+4% (KPa)	OMC-4% WET TO OMC (KPa)	OMC-4% WET TO OMC+4% (KPa)	OMC DRY TO OMC-4% (KPa)	OMC+4% DRY TO OMC (KPa)	OMC+4 DRY TO OMC-4% (KPa)
0	89.073	89.749	89.734	89.706	89.69	89.718	89.635	88.664	89.69
10.16	-6.534	-6.131	-6.143	-6.144	-6.13	-6.129	-5.887	-6.039	-6.13
10.1625	6.284	6.608	6.6	6.601	6.613	6.613	-5.897	6.629	6.613
25.4	1.94	1.958	1.743	2.039	2.077	2.032	2.042	2.085	2.077
25.4025	0.308	0.469	1.994	0.453	0.5	0.486	2.042	0.516	0.5
40.64	0.401	0.348	0.439	0.235	0.322	0.311	0.315	0.324	0.322
40.6425	-0.281	-0.345	0.224	-0.451	-0.348	-0.354	0.315	-0.344	-0.348
71.12	-2.502	-0.14	-0.457	-4.139	-3.825	-0.14	-3.8	-3.822	-3.825
71.1225	-0.188	-0.145	0.137	0.138	-0.145	-0.145	-3.801	-0.144	-0.145
106.68	-0.071	-0.054	0.063	0.063	-0.054	-0.055	-0.054	-0.054	-0.054

Table 10
Variation of the vertical strain with depth.

Vertical coordinates (Depth) cm	OMC (mm)	OMC+4% (mm)	OMC-4% (mm)	OMC WET TO OMC+4% (mm)	OMC-4% WET TO OMC (mm)	OMC-4% WET TO OMC+4% (mm)	OMC DRY TO OMC-4% (mm)	OMC+4% DRY TO OMC (mm)	OMC+4 DRY TO OMC-4% (mm)
0	2.79E-04	2.78E-04	2.78E-04	2.78E-04	2.78E-04	2.78E-04	2.78E-04	2.75E-04	2.78E-04
10.16	1.88E-04	1.87E-04	1.87E-04	1.87E-04	1.87E-04	1.87E-04	1.87E-04	1.86E-04	1.87E-04
10.1625	2.27E-04	2.26E-04	2.26E-04	2.26E-04	2.26E-04	2.26E-04	1.87E-04	2.25E-04	2.26E-04
25.4	7.87E-05	7.78E-05	8.39E-05	7.77E-05	7.77E-05	7.77E-05	7.77E-05	7.75E-05	7.77E-05
25.4025	6.53E-05	6.53E-05	7.78E-05	6.45E-05	6.44E-05	6.47E-05	7.77E-05	6.42E-05	6.44E-05
40.64	2.78E-05	2.72E-05	6.48E-05	2.70E-05	2.69E-05	2.70E-05	2.69E-05	2.69E-05	2.69E-05
40.6425	2.39E-05	2.33E-05	2.71E-05	2.32E-05	2.32E-05	2.33E-05	2.69E-05	2.31E-05	2.32E-05
71.12	1.01E-05	2.56E-05	2.34E-05	1.15E-05	1.10E-05	2.56E-05	1.10E-05	1.10E-05	1.10E-05
71.1225	1.96E-05	2.63E-05	2.24E-05	2.24E-05	2.62E-05	2.63E-05	1.10E-05	2.62E-05	2.62E-05
106.68	9.10E-06	1.28E-05	1.20E-05	1.20E-05	1.28E-05	1.28E-05	1.28E-05	1.28E-05	1.28E-05

Table 11
Variation of the major principal strain with depth.

Vertical coordinates (Depth) cm	OMC (mm)	OMC+4% (mm)	OMC-4% (mm)	OMC WET TO OMC+4% (mm)	OMC-4% WET TO OMC (mm)	OMC-4% WET TO OMC+4% (mm)	OMC DRY TO OMC-4% (mm)	OMC+4% DRY TO OMC (mm)	OMC+4 DRY TO OMC-4% (mm)
0	1.58E-04	1.60E-04	1.60E-04	1.60E-04	1.60E-04	1.60E-04	1.60E-04	1.59E-04	1.60E-04
10.16	-5.32E-05	-5.21E-05	-5.22E-05	-5.22E-05	-5.21E-05	-5.21E-05	-5.15E-05	-5.20E-05	-5.21E-05
10.1625	-5.32E-05	-5.21E-05	-5.22E-05	-5.22E-05	-5.21E-05	-5.21E-05	-5.15E-05	-5.20E-05	-5.21E-05
25.4	-1.90E-05	-1.87E-05	-2.11E-05	-1.85E-05	-1.84E-05	-1.85E-05	-1.85E-05	-1.84E-05	-1.84E-05
25.4025	-1.90E-05	-1.87E-05	-1.86E-05	-1.85E-05	-1.84E-05	-1.85E-05	-1.85E-05	-1.84E-05	-1.84E-05
40.64	-7.59E-06	-7.51E-06	-1.86E-05	-7.66E-06	-7.47E-06	-7.53E-06	-7.49E-06	-7.47E-06	-7.47E-06
40.6425	-7.59E-06	-7.51E-06	-7.71E-06	-7.66E-06	-7.47E-06	-7.53E-06	-7.49E-06	-7.47E-06	-7.47E-06
71.12	-6.81E-06	-8.90E-06	-7.71E-06	-9.74E-06	-9.11E-06	-8.89E-06	-9.06E-06	-9.11E-06	-9.11E-06
71.1225	-6.81E-06	-9.14E-06	-9.77E-06	-9.74E-06	-9.11E-06	-9.14E-06	-9.06E-06	-9.11E-06	-9.11E-06
106.68	-3.08E-06	-4.31E-06	-5.27E-06	-5.26E-06	-4.30E-06	-4.31E-06	-4.30E-06	-4.30E-06	-4.30E-06

Table 12
Variation of the minor principal strain with depth.

Vertical coordinates (Depth) cm	OMC (mm)	OMC+4% (mm)	OMC-4% (mm)	OMC WET TO OMC+4% (mm)	OMC-4% WET TO OMC (mm)	OMC-4% WET TO OMC+4% (mm)	OMC DRY TO OMC-4% (mm)	OMC+4% DRY TO OMC (mm)	OMC+4 DRY TO OMC-4% (mm)
0	1.58E-04	1.60E-04	1.60E-04	1.60E-04	1.60E-04	1.60E-04	1.60E-04	1.59E-04	1.60E-04
10.16	-5.32E-05	-5.21E-05	-5.22E-05	-5.22E-05	-5.21E-05	-5.21E-05	-5.15E-05	-5.20E-05	-5.21E-05
10.1625	-5.32E-05	-5.21E-05	-5.22E-05	-5.22E-05	-5.21E-05	-5.21E-05	-5.15E-05	-5.20E-05	-5.21E-05
25.4	-1.90E-05	-1.87E-05	-2.11E-05	-1.85E-05	-1.84E-05	-1.85E-05	-1.85E-05	-1.84E-05	-1.84E-05
25.4025	-1.90E-05	-1.87E-05	-1.86E-05	-1.85E-05	-1.84E-05	-1.85E-05	-1.85E-05	-1.84E-05	-1.84E-05
40.64	-7.59E-06	-7.51E-06	-1.86E-05	-7.66E-06	-7.47E-06	-7.53E-06	-7.49E-06	-7.47E-06	-7.47E-06
40.6425	-7.59E-06	-7.51E-06	-7.71E-06	-7.66E-06	-7.47E-06	-7.53E-06	-7.49E-06	-7.47E-06	-7.47E-06
71.12	-6.81E-06	-8.90E-06	-7.71E-06	-9.74E-06	-9.11E-06	-8.89E-06	-9.06E-06	-9.11E-06	-9.11E-06
71.1225	-6.81E-06	-9.14E-06	-9.77E-06	-9.74E-06	-9.11E-06	-9.14E-06	-9.06E-06	-9.11E-06	-9.11E-06
106.68	-3.08E-06	-4.31E-06	-5.27E-06	-5.26E-06	-4.30E-06	-4.31E-06	-4.30E-06	-4.30E-06	-4.30E-06

4. Conclusion

A laboratory experiment was carried out on sandy clay to understand the M_R and ε_p behaviour considering wetting and drying under repeated loadings. The repeated loadings were simulated using AASHTO T307 test protocols. M_R and ε_p were determined. M_R and ε_p of the samples were compared. M_R and ε_p models were used to predict M_R and ε_p respectively. A non-linear analysis using KENLAYER software was used to model a hypothetical pavement structure to assess the effect of wetting and drying on pavement performance. Based on this study, the following conclusions were drawn.

1. M_R was high for samples prepared at the OMC and low ε_p. Wetting and drying were shown to have a significant impact on the M_R and ε_p. Specimen subjected to drying process had higher M_R. Higher M_R consistently did not show lower ε_p. The extent of increase and decrease in M_R and ε_p after wetting and drying are dependent on the initial moisture contents. A correlation between M_R and ε_p showed that M_R is not a satisfactory property to explain the ε_p. It is therefore imperative within analytical pavement design protocols to confirm that material parameters and models of material performance have been characterized under conditions that adequately reflect those found in the in-situ conditions considering wetting and drying. Hence, it is recommended that the M_R and ε_p behavior of sandy clayey subgrade soils are investigated considering the wetting, and drying behaviour before making a decision on the final design values.
2. Soil suction represents the combined effects of forces holding water, it provides the basis that reflects on the M_R and ε_p behaviour and its characteristics. Suction hysteresis results in the difference between suction on the drying and

wetting curves. Hence, the hysteresis observed in suction measurement better explains the effect of the wetting and drying condition on M_R and ε_p.

3. Three models were used [10,41], and [42] to predict stress state effect on M_R under varying wetting and drying conditions. A comparison of the performance of the three models, [42] showed a better performance considering all the conditions (wetting, drying and compaction moisture content).
4. The effect of drying and wetting has the potential to instigate the cause of rutting failure by fatigue cracking and permanent deformation in flexible pavements.

In future, the drying and wetting effect on M_R and ε_p will be assessed considering suction measurement. Further, the study was limited to Ciyaowan station in Bao-Shen. Future studies will involve evaluating the effect of the drying and wetting on M_R and ε_p for other soils.

Acknowledgement

This project was supported by the National Natural Science Foundation of China (51478279), Natural Science Foundation of Hebei Province (E2019210137). These financial supports are gratefully acknowledged.

Funding

This project was supported by the National Natural Science Foundation of China (51478279), Natural Science Foundation of Hebei Province (E2019210137). These financial supports are gratefully acknowledged. The Earthworks engineers stationed in Ciyaowan station in Bao-shen reported several subgrade related problems. To remedy the problem, a joint study was conducted with the state department and Shijiazhuang Tiedao Railway University. Results reported here are part of the several laboratory tests conducted.

Conflicts of interest/Competing interests

The authors declare the following National Natural Science Foundation of China, Natural Science Foundation of Hebei Province, Shijiazhuang Tiedao University and Hebei State depart of Earthworks engineers as the potential competing interests.

References

[1] M. Y. Abu-Farsakh, A. Mehrotra, L. Mohammad, K. Gaspard, Incorporating the effect of moisture variation on resilient modulus for unsaturated fine-grained subgrade soils, Transp. Res. Rec. 2510 (1) (2015) 44–53.

[2] N. Khoury, R. Brooks, M. M. Zaman, C. N. Khoury, Variations of resilient modulus of subgrade soils with postcompaction moisture contents, Transp. Res. Rec. 2101 (1) (2009) 72–81.

[3] K. Naji, Resilient modulus–moisture content relationships for pavement engineering applications, Inter. J. Pavement Eng. 19 (7) (2018) 651–660.

[4] A. J. Puppala, S. Saride, S. Chomtid, Experimental and modeling studies of permanent strains of subgrade soils, J. Geotech. Geoenvironmental Eng. 135 (10) (2009) 1379–1389.

[5] P. Ullidtz, Mathematical model of pavement performance under moving wheel load, Transp. Res. Rec. 1384 (1) (1993) 94–99.

[6] N. Venkatesh, M. Heeralal, R. J. Pillai, Resilient and permanent deformation behaviour of clayey subgrade soil subjected to repeated load triaxial tests, Eur. J. Environ. Civ. Eng. 24 (9) (2020) 1414-1429.

[7] M. A. Khasawneh, Permanent deformation behavior of cohesive subgrade soils classified as A-4a and A-6a, Mater. Today Proc. (2020) https://www.sciencedirect.com/science/article/pii/S2214785 32033529X

[8] R. Chen, J. Chen, X. Zhao, X. Bian, Y. Chen, Cumulative settlement of track subgrade in high-speed railway under varying water levels, Inter. J. Rail Transp. 2 (4) (2014) 205–220.

[9] A. J. Ceratti, W. Y. Y. Gehling, W. P. Núñez, Seasonal variations of a subgrade soil resilient modulus in southern Brazil, Transp. Res. Rec. 1874 (1) (2004) 165–173.

[10] J. Zhang, J. Peng, J. Zheng, Y. Yao, Characterisation of stress and moisture-dependent resilient behaviour for compacted clays in South China, Road Mater. Pavement Des. 21 (1) (2020) 262–275.

[11] T. Pan, E. Tutumluer, J. Anochie-Boateng, Aggregate morphology affecting resilient behavior of unbound granular materials, Transp. Res. Rec. 1952 (1) (2006) 12–20.

[12] D. Andrei, M. W. Witczak, C. W. Schwartz, J. Uzan, Harmonized resilient modulus test method for unbound pavement materials, Transp. Res. Rec. 1874 (2004) (1) 29–37.

[13] X. Liu, X. Zhang, H. Wang, B. Jiang, Laboratory testing and analysis of dynamic and static resilient modulus of subgrade soil under various influencing factors, Constr. Build. Mater. 195 (2019) 178–186.

[14] C. E. Cary and C. E. Zapata, Enhancement of the model for resilient response of soils due to seasonal environmental changes implemented in the M-EPDG, Transp. Res. Rec. 2170 (2010) 36–44.

[15] Y. Qiao, G. W. Flintsch, A. R. Dawson, T. Parry, Examining effects of climatic factors on flexible pavement performance and service life, Transp. Res. Rec. 2349 (1) (2013) 100–107.

[16] Y. Ali, M. Irfan, M. Zeeshan, I. Hafeez, S. Ahmed, Revisiting the relationship of dynamic and resilient modulus test for asphaltic concrete mixtures, Constr. Build. Mater. 170 (2018) 698–707.

[17] A. Sawangsuriya, T. B. Edil, P. J. Bosscher, Modulus-suction- moisture relationship for compacted soils, Can. Geotech. J. 45 (7) (2008) 973–983.

[18] H. Yuan, W. Li, Y. Wang, H. Lin, Y. Liu, Resilient Modulus—Physical Parameters Relationship of Improved Red Clay by Dynamic Tri-Axial Test, Appl. Sci. 9 (6) (2019) 1155.

[19] L.-S. Huang and Y. V. Kang, Nondestructive evaluation of thickness and bearing capacity of roadway pavement structure, Inter. J. Pavement Res. Technol. 3 (6) (2010 326-335.

[20] M. S. Hossain, Estimation of subgrade resilient modulus for Virginia soil, Transp. Res. Rec. 2101 (1) (2009) 98–109.

[21] E. Pan, E. Chen, W. Alkasawneh, Layered flexible pavement studies: challenges in forward and inverse problems, Inter. J. Pavement Res. Technol. 1 (1) (2008) 12–16.

[22] F. Lekarp, U. Isacsson, A. Dawson, State of the art. II: Permanent strain response of unbound aggregates, J. Transp. Eng. 126 (1) (2000) 76–83.
[23] M. H. Lal, V. Noolu, R. J. Pillai) Kurre, G. V. Praveen, A review on permanent deformation of granular material, Indian J. Public Health Res. Dev. 9 (11) (2018) 1158–1165.
[24] Z. Wu and X. Chen, Prediction of permanent deformation of pavement base and subgrade materials under accelerated loading, Inter. J. Pavement Res. Technol. 4 (4) (2011) 231-237.
[25] A. Alnedawi, K. P. Nepal, R. Al-Ameri, Effect of loading frequencies on permanent deformation of unbound granular materials, Inter. J. Pavement Eng. (2019) https://doi.org/10.1080/10298436.2019.1656807
[26] Z. Luo, C.-S. Ku, L. Bu, Probabilistic model for long-term deformation of subgrade soil in upgrading-speed railway lines, Inter. J. Pavement Res. Technol. 4 (1) (2011) 34-40.
[27] T. Y. Elkady, A. M. Al-Mahbashi, M. A. Al-Shamrani, Effect of moisture hysteresis on the resilient modulus of lime-treated expansive clay, J. Test. Eval. 45 (6) (2017) 2039–2049.
[28] C. L. Monismith, N. Ogawa, C. R. Freeme, Permanent deformation characteristics of subgrade soils due to repeated loading, Transp. Res. Rec. 537 (1975) 1-17.
[29] N. N. Khoury, M. M. Zaman, Correlation between resilient modulus, moisture variation, and soil suction for subgrade soils, Transp. Res. Rec. 1874 (1) (2004) 99–107.
[30] A. J. Puppala, L. N. Mohammad, A. Allen, Permanent deformation characterization of subgrade soils from RLT test, J. Mater. Civ. Eng. 11 (4) (1999) 274–282.
[31] E. E. Alonso, N. M. Pinyol, A. Gens, Compacted soil behaviour: initial state, structure and constitutive modelling, Géotechnique 63 (6) (2013) 463.
[32] D. Cheng, Z. Guo-yong, L. Wen-jie, Z. Lun, Z. Rui-lei, Improved Prediction Model for Dynamic Resilient Modulus of Subgrade Silty Clay in Eastern Hunan and Its Relevant Finite Element Method Implementation, Am. J. Civ. Eng. 6 (1) (2018) 44.
[33] D. G. Fredlund, A. Xing, S. Huang, Predicting the permeability function for unsaturated soils using the soil-water characteristic curve, Can. Geotech. J. 31 (4) (1994) 533–546.
[34] E. C. Drumm, J. S. Reeves, M. R. Madgett, W. D. Trolinger, Subgrade resilient modulus correction for saturation effects, J. Geotech. Geoenvironmental Eng. 123 (7) (1997) 663–670.
[35] A. Sawangsuriya, T. B. Edil, C. H. Benson, Effect of suction on resilient modulus of compacted fine-grained subgrade soils, Transp. Res. Rec. 2101 (1) (2009) 82–87.
[36] N. Perez-Garcia, D. Fredlund) Garnica-Anguas, N. Mestas-Martinez, A model to predict changes in resilient modulus resulting from wetting and drying, Infraestruct. Vial 17 (30) (2015) 23–30.
[37] Z. Han and S. K. Vanapalli, Model for predicting resilient modulus of unsaturated subgrade soil using soil-water characteristic curve, Can. Geotech. J. 52 (10) (2015) 1605–1619.
[38] M. M. Rahman, S. L. Gassman, Permanent Deformation Characteristics of Coarse Grained Subgrade Soils Using Repeated Load Triaxial Tests, Geo-Congress 2019: Geotechnical Materials, Modeling, and Testing American Society of Civil Engineers, Reston, VA, USA, 2019.
[39] J. Peng, J. Zhang, J. Li, Y. Yao, A. Zhang, Modeling humidity and stress-dependent subgrade soils in flexible pavements, Comput. Geotech. 120 (2020) 103413.
[40] Y. H. Huang, Pavement analysis and design, Perason Prentice Hall, Kentucky, USA, 2004.
[41] J. Uzan, Characterization of clayey subgrade materials for mechanistic design of flexible pavements, Transp. Res. Rec. 1629 (1) (1998) 189–196.
[42] B. Ni, T. C. Hopkins, L. Sun, T. L. Beckham, Modeling the resilient modulus of soils, Proc. 6th International Conference on The Bearing Capacity of Roads And Airfields, Lisbon, Portugal, vol. 2, 2002.